Resistance jumps in mercury injection in porous media

Jean-Noel Roux* and David Wilkinson
Schlumberger-Doll Research, Old Quarry Road, Ridgefield, Connecticut 06877-4108
(Received 8 October 1987)

Recent experiments by A. H. Thompson, A. J. Katz, and R. A. Raschke [Phys. Rev. Lett. **58**, 29 (1987)] have demonstrated that, when mercury is injected into a porous material, the electrical resistance of the sample decreases in a stepwise manner, with a power-law distribution of step sizes. Here we present computer simulations and a theoretical analysis of this process based on the model of invasion percolation. The simulations are consistent with the prediction that the number N of resistance steps greater in size than a given ΔR should scale as $(\Delta R)^{-\lambda}$, with λ given in terms of the conduction exponent t and correlation-length exponent ν by $3\nu/(t+3\nu)$. This gives $\lambda \sim 0.58$, somewhat smaller than the experimental value 0.81 given by Thompson, Katz, and Raschke. It is argued that neither the resistance jumps themselves nor the hysteresis and long relaxation times observed in the experiment provide evidence against the application of percolation theory to fluid displacement in porous media. From the viewpoint of computer simulation, it is suggested that measurement of the exponent λ may be a good way of obtaining the value of the conduction exponent t.

I. INTRODUCTION

One of the standard ways of characterizing porous materials is mercury porosimetry. In this process, mercury is injected into an evacuated sample and enters the pores of the material by overcoming the capillary resistance due to surface tension. If we idealize the pores as cylinders, then the mercury pressure (capillary pressure) $p_{\rm cap}$ required to enter a pore of radius r is

$$p_{\rm cap}=\frac{2\gamma\cos\theta}{r}\ , \tag{1}$$

where γ is the interfacial tension and θ is the contact angle. Because naturally occurring porous media are disordered, the radius, and hence the mercury pressure needed for penetration, varies from pore to pore, and so a plot of mercury saturation (fraction of the pore space occupied by mercury) against pressure gives a measure of the pore-size distribution of the material.

This simple picture is complicated by percolation effects, the importance of which in fluid-fluid displacements has been recognized by many authors.[1–11] At any given mercury pressure $p_{\rm cap}$, a certain fraction p of pores are large enough that they can be penetrated by the mercury. However not all such pores will actually be filled, but only those to which there exists a connected path of occupied pores. Thus we have a percolation picture in which the occupation fraction p is in one-to-one correspondence with the capillary pressure $p_{\rm cap}$, but the mercury only occupies the "infinite" cluster which is connected to the inlet face(s) of the sample—"finite" disconnected clusters are not occupied.

More detailed information about the system may be obtained by measuring the electrical resistance of the sample as the mercury injection proceeds. A very careful experiment of this type has recently been performed by Thompson, Katz, and Raschke,[12] hereafter denoted by TKR. In this experiment, the mercury was injected from one face of the sample, and the electrical resistance measured between this and the opposite face with a two-electrode system. When the pressure was increased in small increments, it was found that the resistance decreased in a stepwise manner, with a power-law distribution of step sizes.

The purpose of the present paper is to perform computer simulations of the resistance step phenomenon, and to present a scaling analysis which is motivated by, but somewhat different from, that of TKR. This work is presented in Sec. II. In Sec. III, we discuss these results and consider whether they are consistent with a percolation picture of the injection process.

II. THEORETICAL MODEL

The theoretical model which we employ is essentially that of invasion percolation.[3,4,7–10] In this model, the porous medium is represented as a lattice in which the bonds represent pores. Each bond is assigned a random number representing the pressure at which it will fill with the displacing fluid. Initially the displacing fluid occupies one face (the inlet face) of the lattice, and the displacing fluid advances at each time step by occupying the available bond with the smallest random number. The invasion percolation algorithm is actually a kinetic growth process, and makes no reference to the occupation fraction. The original physical motivation for the algorithm was to provide a unique sequence of events—this is particularly important when considering the effects of "trapping" of the displaced phase.[3,4,7–10] Here, however, since the displaced phase is a vacuum the distinction between invasion percolation and normal percolation is not so crucial, and we will use the following algorithm.

(1) At each time step the pressure is increased until an accessible bond can be filled. If this accesses additional bonds which can be filled at that pressure, then they are filled also.

(2) When no more bonds can be filled at the current value of the pressure, the end-to-end electrical resistance of the configuration is computed by inversion of the conductance matrix.

The main feature of this algorithm is that at any pressure (occupation fraction) the mercury configuration is the same as that which would be obtained by constructing the corresponding percolation configuration, and then keeping only those mercury clusters which are connected to the inlet face of the sample. This has two important consequences:

(1) The occupation fraction has a rather different interpretation from that in ordinary percolation. Rather than being the actual fraction of occupied bonds, it is the fraction which could be occupied if all bonds were accessible to the mercury.

(2) At a given occupation fraction, the electrical conductance, which comes only from the spanning cluster, is exactly the same as in ordinary percolation. In particular, when the pressure is such that the occupation fraction p is below the percolation threshold p_c, there is no spanning cluster and the electrical resistance is infinite.

Our computer simulations are performed on an $L \times L \times L$ simple cubic lattice, for which the bond percolation threshold is at $p_c \sim 0.247$. The size L of the lattice is typically taken in the range $15 \leq L \leq 20$. Periodic boundary conditions are applied in the transverse y and z directions, while the ends of the network at $x=0$ and $x=L$ are linked to "bus bars"—plane electrodes between which a unit current is imposed in order to compute the conductance of the system. Each bond is a cylinder, of fixed length l, whose radius r has been drawn at random from a uniform distribution in an interval $[r_{\min}, r_{\max}]$. This distribution may be achieved by assigning to each bond a random number q, uniformly distributed on the interval [0,1], with q and r related by

$$q = \frac{r_{\max} - r}{r_{\max} - r_{\min}} . \tag{2}$$

Filling the largest accessible pore thus corresponds to selecting the smallest random number q. At any stage in the simulation, we identify the occupation fraction p as the largest q value selected up to that point. When it is filled with mercury, the conductance g of a bond is assumed to be proportional to the cross-sectional area

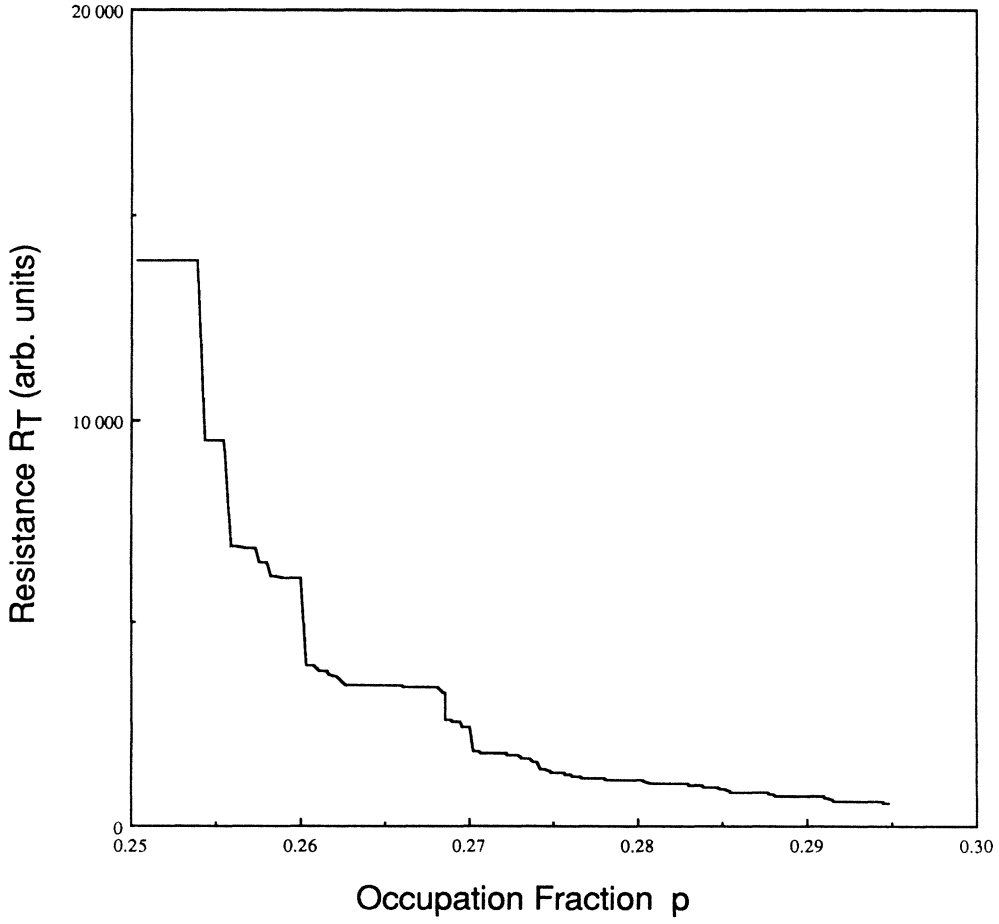

FIG. 1. Plot of the total sample resistance R_T against occupation fraction p for a single realization on a system of size $L=20$. Note that below the percolation threshold $p_c \sim 0.247$ the resistance is infinite.

$$g \sim r^2 . \tag{3}$$

In practice, we have chosen the ratio r_{max}/r_{min} to be equal to 2. This is, of course, somewhat arbitrary but the critical behavior, by virtue of its universality, should not be sensitive to this particular choice, or to the assumption of a uniform distribution.

In Fig. 1 we plot the sample resistance R_T as a function of the occupation fraction p for a single realization of size $L=20$. As in the experiment of TKR, we see a large number of steps, with a wide range of step sizes. In Fig. 2 we plot the same information as a log-log plot of resistance against $\epsilon=p-p_c$. Despite the jumps, we see that on the average the plot for small ϵ is a straight line showing the usual critical behavior of percolation conduction. The obtained value 1.87 for the conduction exponent t is in excellent agreement with the accepted value of 1.9.

Following TKR, in Fig. 3 we plot the number N of resistance jumps greater than a given ΔR_T against ΔR_T. We see that over a wide range of ΔR_T the data follow a power law $N \sim (\Delta R_T)^{-\lambda}$. Depending on which values of ΔR_T are used in the fit, we obtain exponent values λ in the range 0.55 to 0.63, the latter probably being more representative of the critical region. Similar results were obtained on another realization of size $L=20$, and on two realizations of size $L=15$.

Our theoretical scaling argument for the above behavior is based on that given by TKR. Let us consider a time in the simulation or experiment where the occupation fraction is p and the correlation length is $\xi \sim \epsilon^{-\nu}$, where $\epsilon=p-p_c$. It is convenient to consider the system to be made up of $(L/\xi)^3$ subsystems of linear extent ξ. Each of the subsystems has a resistance R of order

$$R \sim \frac{\rho}{\xi} , \tag{4}$$

with the resistivity ρ scaling as

$$\rho \sim \epsilon^{-t} , \tag{5}$$

where t is the conduction exponent. In general, an infinitesimal increase in the occupation fraction will change the configuration (and hence resistance) of at most one of these regions. Thus we will assume that the observed macroscopic resistance jumps are due to those increases in the occupation fraction which cause a significant change in the resistance of just one of these subsystems. On average, in a given subsystem such a change will only occur when the occupation fraction p is changed by an amount δp of order ϵ. This may be seen by considering the number of singly connected bonds in such a subsystem, which scales as ϵ^{-1}.[13,14] The change in the resistance of the subsystem is thus

$$\Delta R \sim \frac{1}{\xi}\frac{d\rho}{dp}\delta p \sim \frac{1}{\xi}\epsilon^{-t} , \tag{6}$$

i.e., it is of the same order as the resistance R itself. Following TKR, we may use Cohn's theorem[15,16] to obtain

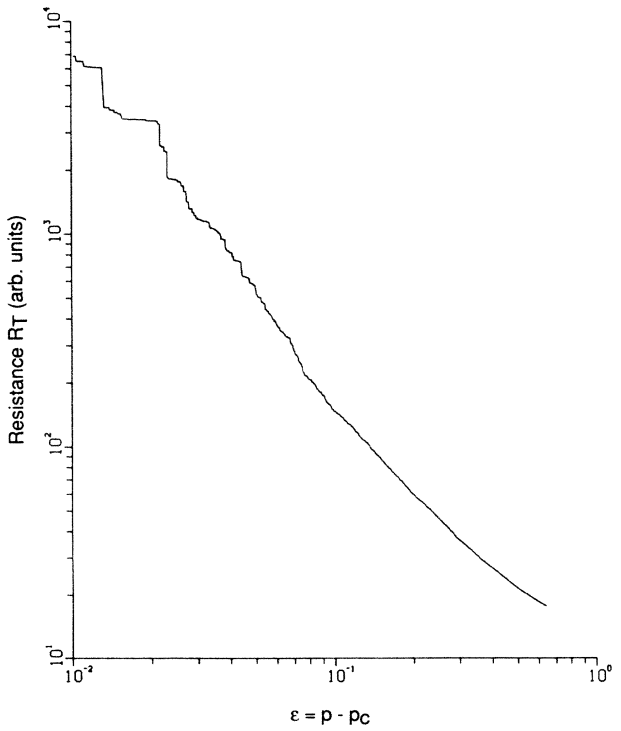

FIG. 2. Log-log plot of the total sample resistance R_T against $\epsilon=p-p_c$ for the same realization as in Fig. 1. Note that below $\epsilon \sim 10^{-1}$ the smoothed curve follows a power law $R_T \sim \epsilon^{-t}$ with exponent $t \sim 1.87$.

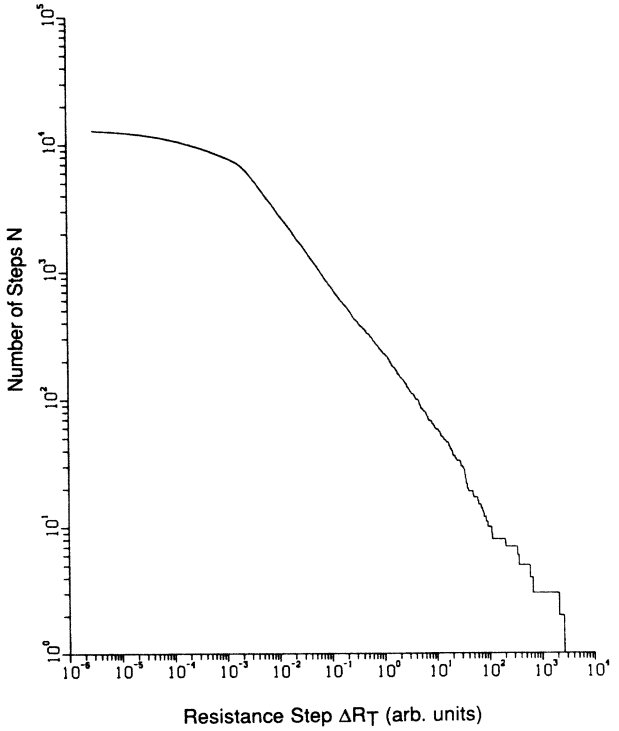

FIG. 3. Log-log plot of the number N of resistance jumps greater than ΔR_T against ΔR_T for the same realization as in Fig. 1. The plot indicates a power law $N \sim (\Delta R_T)^{-\lambda}$ with λ between 0.55 and 0.63, depending on exactly which range of ΔR_T values are used in the fit.

the corresponding change in the resistance of the entire system as

$$\Delta R_T \sim \left[\frac{\xi}{L}\right]^4 \Delta R \sim \frac{\xi^3}{L^4}\epsilon^{-t} \sim \frac{1}{L^4}\epsilon^{-(t+3\nu)} . \tag{7}$$

Now an increase δp of order ϵ will cause such a change in *each* of the $(L/\xi)^3$ subsystems, so on average the change Δp required to produce *one* such change is

$$\Delta p \sim \left[\frac{\xi}{L}\right]^3 \delta p \sim \left[\frac{\xi}{L}\right]^3 \epsilon . \tag{8}$$

Thus the total number of jumps larger than ΔR_T scales as

$$N \sim \int_{p_c}^{p} \frac{dp}{\Delta p} \sim L^3 \epsilon^{3\nu} . \tag{9}$$

Eliminating ϵ between (7) and (9) yields

$$N \sim L^{3(t-\nu)/(t+3\nu)} (\Delta R_T)^{-\lambda} , \tag{10}$$

where the exponent λ is given by

$$\lambda = \frac{3\nu}{t+3\nu} . \tag{11}$$

Using $\nu \sim 0.88$ and $t \sim 1.9$ gives $\lambda \sim 0.58$, in excellent agreement with the value between 0.55 and 0.63 obtained in our simulations.

Although this derivation is based on that of TKR, there are some significant differences. Firstly, we explicitly calculate in (8) the change Δp in the occupation fraction required to bring about a single resistance jump—this was not done by TKR, and this would appear to be the main reason why our obtained value of λ is different from the theoretical value 0.75 obtained by them. It should be emphasized that the change Δp has nothing to do with the actual experimental increments in the occupation fraction, which are assumed infinitesimal; rather it is the average amount by which p must be increased in order to bring about a "significant" change in the resistance in a single region of linear extent ξ. If we rewrite (8) in the form

$$\Delta p \sim \frac{1}{L^3}\epsilon^{1-3\nu} , \tag{12}$$

we see that Δp decreases as ϵ increases. The apparent divergence at small ϵ is cut off by finite-size effects at $\epsilon \sim L^{-1/\nu}$ to give a maximum value

$$\Delta p_{\max} \sim L^{-1/\nu} . \tag{13}$$

If the experimental pressure changes are such as to cause the occupation fraction to change by an amount Δp_{expt} which is large compared to $\Delta p_{\max}$ then the above steps will not be seen, but instead we will see steps obtained by "sampling" the macroscopic resistance curve

$$R_T \sim \frac{\rho}{L} , \tag{14}$$

with the resistivity ρ given by the critical behavior (5). When ρ is changed by an amount Δp_{expt} this resistivity changes by an amount

$$\Delta R_T \sim \frac{1}{L}\frac{d\rho}{dp}\Delta p_{\text{expt}} \sim \frac{\Delta p_{\text{expt}}}{L}\epsilon^{-(1+t)} . \tag{15}$$

The number of jumps larger than this ΔR_T scales as

$$N \sim \int_{p_c}^{p} \frac{dp}{\Delta p_{\text{expt}}} \sim \frac{\epsilon}{\Delta p_{\text{expt}}} . \tag{16}$$

Eliminating ϵ between (15) and (16) yields

$$N \sim L^{-1/(t+1)} (\Delta p_{\text{expt}})^{-t/(t+1)} (\Delta R_T)^{-\lambda} , \tag{17}$$

where the exponent λ is now given by

$$\lambda = \frac{1}{t+1} \sim 0.34 , \tag{18}$$

where we have used the value $t = 1.9$. For intermediate values of the pressure increment, a crossover between the behaviors (11) and (18) will be seen. An example of this kind of behavior is seen in Fig. 4.

A second difference from the TKR derivation is that, despite the observed resistance jumps, the total sample resistance in our model has the property that it follows the percolation critical behavior on the average. To see this, we observe that if indeed we assume that the total resistance R_T satisfies (14), then under a change Δp as in (8) the resistance changes by an amount

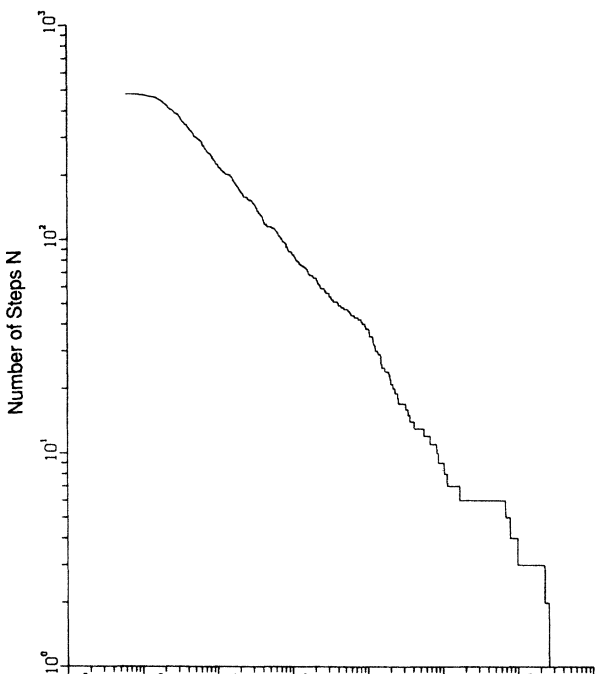

FIG. 4. Log-log plot of the number N of resistance jumps greater than ΔR_T against ΔR_T for a case showing the crossover between the behaviors (11) and (18). This case was obtained by increasing the mercury pressure by a fixed amount at each step; close to the percolation threshold this corresponded to an increase in the occupation fraction $\Delta p_{\text{expt}} \sim 2 \times 10^{-3}$. The slopes of the two straight-line portions give values for λ of 0.61 and 0.41, in reasonable agreement with the predicted values 0.58 and 0.34.

$$\Delta R_T \sim \frac{1}{L}\frac{dp}{dp}\Delta p \sim \frac{\xi^3}{L^4}\epsilon^{-t} . \tag{19}$$

This is the same as our relation (7), thus demonstrating that the sum total of the jumps is just such as to cause the sample resistance to "track" the curve (14).

One feature of our derivation, common also to that of TKR, is the assumption that the size of the jumps is controlled by the current value of ϵ, so that larger jumps occur before smaller ones. This, of course, is not strictly true, but it is reasonable to expect the above to give the correct scaling relation for the number of jumps greater than a given size. We have attempted to further verify the scaling derivation by checking the L dependence given in (10). However, with only a few realizations the data seem too noisy to do this reliably. It should be emphasized that these simulations are extremely time consuming, since they require inversion of the conductance matrix after every step.

III. DISCUSSION

The main result of this paper is that simulations of mercury injection based on the model of invasion percolation do lead to resistance steps with a power-law distribution of resistances, as found in the experiments of Thompson, Katz, and Raschke. In addition we have presented a scaling argument for the exponent λ which gives $\lambda = 3\nu/(t+3\nu) \sim 0.58$, which is in excellent agreement with the value between 0.55 and 0.63 found in our simulations, but somewhat smaller than the value 0.81 found in the experiments of TKR. We have also shown that when the experimental increments in the mercury pressure are too large, there is a crossover to a different behavior with $\lambda = 1/(t+1) \sim 0.34$. It should be emphasized that all the conclusions of this paper are based on a *theoretical model* of the mercury injection process. In common with all other applications of percolation theory to immiscible displacement in porous media (including the theoretical analysis of TKR), this model is founded on the physical idea of a one-to-one correspondence between capillary pressure and occupation fraction. For this reason these terms have been used interchangeably in this paper. The purpose of the paper was to give a correct analysis of the resistance step phenomenon based on this theoretical model. As such, the paper is essentially a theoretical analysis of percolation conduction, and cannot provide an explanation for the discrepancy between the experimental and theoretical values of the exponents. The origin of this discrepancy is not clear. One possibility is that the experiment is not really operating in the critical region. However, our simulations show a power-law behavior over a very wide range of step sizes, with an exponent which if anything decreases as we move out of the critical region.

TKR interpret the experimental resistance jumps as evidence for the breakdown of percolation theory as a model for the injection process. We do not agree with this interpretation. One of the main features of our theoretical picture is that, despite the resistance jumps, if the graph of total resistance R_T against pressure (occupation fraction) is smoothed, then it follows the usual percolation critical behavior

$$R_T \sim \frac{1}{L}\epsilon^{-t} . \tag{20}$$

This has to be the case, because the spanning cluster in the model is exactly the same as that in ordinary percolation theory at the same occupation fraction. Percolation theory is called a second-order phase transition because the order parameter, which here is the mercury saturation, is a continuous function of the pressure (occupation fraction) with a discontinuous derivative. Viewed in terms of the conductivity, the transition is third order because the first derivative is also continuous (the conduction exponent t is greater than unity). Both these terminologies apply to the system in the thermodynamic limit; in our opinion the resistance jumps seen in the experiment of TKR are simply the expected finite-size effects of percolation conduction, and do not indicate first-order behavior in the technical sense.

As further evidence for the suggested breakdown of percolation theory, TKR cite the hysteresis and long relaxation times observed in their experiment. Let us consider each of these observations in turn.

The origins of hysteresis effects in fluid displacements are numerous, but qualitatively well understood. At the level of the solid surface there is contact angle hysteresis. At the pore level[17] the events which cause the pore emptyings in mercury withdrawal (an imbibition process) can occur at different pressures and in a different order from the pore fillings in mercury injection (a drainage process). Even a simple percolation picture in which the pores empty at the same pressure as they filled will lead to hysteresis in the saturation (though not in the electrical resistance) due to the stranding of finite clusters of mercury. When all these effects are put together, the situation can become extremely complicated, but not in such a way as to violate the notion of capillary equilibrium on which percolation models are based. In particular, the existence of hysteresis does not invalidate a simple percolation picture of the initial injection.

The long relaxation times, of the order of hours, observed in the TKR experiment can also have a simple interpretation. Percolation theory alone does not provide a complete model of fluid displacement phenomena, but only a description of the fluid configurations when the system has reached capillary equilibrium. By itself, percolation has nothing to say about the manner in which this equilibrium is reached. In the experiment, the mercury pressure is increased at the inlet face, and mercury begins to enter the medium. Initially the mercury saturation increases only near the inlet, and only after some time do the pressure and saturation reach (statistically) uniform values throughout the sample. Macroscopically, this return to capillary equilibrium following a small pressure increment may be viewed as a diffusion process with diffusion constant

$$D = \frac{k_{\text{merc}}}{\mu\phi}\frac{dp_{\text{cap}}}{dS} , \tag{21}$$

where μ is the mercury viscosity, ϕ is the porosity, k_{merc} is the effective permeability to the mercury at its current equilibrium saturation, and dp_{cap}/dS is the derivative of the capillary pressure with respect to the mercury saturation, again evaluated at the current equilibrium saturation. Close to the percolation threshold, the latter two quantities have the behavior[10]

$$k_{\text{merc}} \sim k\epsilon^t , \tag{22}$$

where k is the absolute permeability, and

$$\frac{dp_{\text{cap}}}{dS} \sim \frac{\gamma}{r}\epsilon^{1-\beta} , \tag{23}$$

where γ is the interfacial tension, r is a microscopic length (e.g., a grain size), and $\beta \sim 0.45$ is the "magnetic" exponent of percolation. For a 10% porosity sample with permeability 100 millidarcies (10^{-9} cm^2) and a grain size of 10 μm, and values $\mu \sim 0.015$ p and $\gamma \sim 500$ dyn/cm we obtain

$$D \sim 0.3\epsilon^{t+1-\beta} \text{ cm}^2/\text{sec} . \tag{24}$$

On a sample of linear extent $L \sim 1$ cm, this gives a characteristic diffusion time

$$\tau \sim \frac{L^2}{D} \sim 3\epsilon^{-(t+1-\beta)} \text{ sec.} \tag{25}$$

For small values of ϵ (say 10^{-2}) this can easily lead to relaxation times of the order of hours.

TKR interpret the long relaxation times, together with the observed hysteresis, as evidence for the existence of metastable states. To some extent, this is certainly true. In mercury injection, the lowest energy state is one in which the mercury occupies the largest pores, irrespective of accessibility. But the nature of the injection process constrains the mercury to occupy a connected cluster—this is precisely why percolation theory is relevant to the process. While perhaps over geological time it is possible for fluids to find their lowest energy configuration, we do not believe that this can happen over the time scale of a mercury porosimetry experiment. Rather, the long relaxation times can be explained as above as being the time required for pressure diffusion to access those configurations which *are* allowed by percolation theory.

Our overall conclusion is that the experimentally observed resistance jumps, hysteresis and long relaxation times are all consistent with a percolation picture of the process. In particular, resistance jumps with a power-law distribution of sizes are seen in a simple percolation model of the primary injection. As a final observation, we may note that from the viewpoint of simulation a measurement of the exponent $\lambda = 3\nu/(t+3\nu)$ may be a good way of estimating the value of the conduction exponent t, since it requires neither knowledge of the percolation threshold nor simulations on lattices of different sizes. Indeed, even without ensemble averaging, our simulation value $\lambda = 0.59$ (midway between our extremes of 0.55 and 0.63) combined with $\nu = 0.88$ gives $t = 1.83$, in good agreement with the currently accepted value of $t = 1.9$.

Note added: As this manuscript was being completed, we learned of similar work by Batrouni, Kahng, and Redner.[18] These authors present a scaling argument giving a resistance step exponent $\lambda = d\nu/(t+3\nu)$ in d dimensions, in agreement with our result for $d = 3$. Monte Carlo simulations in two dimensions are also presented. We thank S. Redner for bringing this work to our attention.

ACKNOWLEDGMENTS

The authors would like to thank J. Banavar, J. Koplik, and T. S. Ramakrishnan for useful discussions.

*Current address: Laboratoire de Physique, Ecole Normale Superieure de Lyon, 46 Allée d'Italie, 69364 Lyon Cedex 07, France.

[1] J. C. Melrose and C. F. Brandner, Can. J. Petrol. Technol. **13**, 54 (1974).
[2] P. G. de Gennes and E. Guyon, J. Mec. **17**, 403 (1978).
[3] R. Lenormand and S. Bories, C. R. Acad. Sci. Paris **291**, 279 (1980).
[4] R. Chandler, J. Koplik, K. Lerman, and J. Willemsen, J. Fluid Mech. **119**, 249 (1982).
[5] R. G. Larson, L. E. Scriven, and H. T. Davis, Chem. Eng. Sci. **36**, 57 (1981).
[6] R. G. Larson and N. R. Morrow, Powder Technol. **30**, 123 (1981).
[7] D. Wilkinson and J. Willemsen, J. Phys. A **16**, 3365 (1983).
[8] D. Wilkinson, Phys. Rev. A **30**, 520 (1984).
[9] J. Willemsen, Phys. Rev. Lett. **52**, 2197 (1984).
[10] D. Wilkinson, Phys. Rev. A **34**, 1380 (1986).
[11] T. S. Ramakrishnan and D. T. Wasan, Int. J. Multiphase Flow **12**, 357 (1986).
[12] A. H. Thompson, A. J. Katz, and R. A. Raschke, Phys. Rev. Lett. **58**, 29 (1987).
[13] A. Coniglio, Phys. Rev. Lett. **46**, 250 (1981).
[14] A. Coniglio, J. Phys. A **15**, 3829 (1982).
[15] R. M. Cohn, Proc. Am. Math. Soc. **1**, 316 (1950).
[16] R. Rammal, C. Tannous, and A.-M. S. Tremblay, Phys. Rev. A **31**, 2662 (1985).
[17] R. Lenormand and C. Zarcone, Society of Petroleum Engineers Report No. 13264, 1984 (unpublished).
[18] G. Batrouni, B. Kahng, and S. Redner, J. Phys. A **21**, L23 (1988).